

Decision-making with Speculative Opponent Models

Jing Sun¹, Shuo Chen^{2*}, Cong Zhang¹, Yining Ma¹, Jie Zhang¹

¹School of Computer Science and Engineering, Nanyang Technological University
Singapore 639798

²Beijing Institute for General Artificial Intelligence,
Beijing, China 100091

{sun.jing, yining.ma, zhangj}@ntu.edu.sg, cong030@e.ntu.edu.sg, chenshuo@bigai.ai

Abstract

Opponent modelling has proven effective in enhancing the decision-making of the controlled agent by constructing models of opponent agents. However, existing methods often rely on access to the observations and actions of opponents, a requirement that is infeasible when such information is either unobservable or challenging to obtain. To address this issue, we introduce Distributional Opponent-aided Multi-agent Actor-Critic (DOMAC), the first speculative opponent modelling algorithm that relies solely on local information (i.e., the controlled agent’s observations, actions, and rewards). Specifically, the actor maintains a speculated belief about the opponents using the tailored *speculative opponent models* that predict the opponents’ actions using only local information. Moreover, DOMAC features distributional critic models that estimate the return distribution of the actor’s policy, yielding a more fine-grained assessment of the actor’s quality. This thus more effectively guides the training of the speculative opponent models that the actor depends upon. Furthermore, we formally derive a policy gradient theorem with the proposed opponent models. Extensive experiments under eight different challenging multi-agent benchmark tasks within the MPE, Pommerman and StarCraft Multiagent Challenge (SMAC) demonstrate that our DOMAC successfully models opponents’ behaviours and delivers superior performance against state-of-the-art methods with a faster convergence speed.

Introduction

Recently, there has been a growing effort in applying multi-agent reinforcement learning (MARL) to address the complex learning tasks in multi-agent systems, including cooperation, competition, and a mix of both (Hernandez-Leal, Kartal, and Taylor 2019; Zhang, Yang, and Başar 2021; Yu et al. 2021; Papoudakis et al. 2020). The framework of centralized training with decentralized execution (CTDE) has drawn enormous attention, where the policy of each agent is trained with access to global information in a centralized way and executed given only the local observations in a decentralized manner. Empowered by CTDE, plenty of multi-agent RL (MARL) methods are proposed (Lowe et al. 2017; Foerster et al. 2018b; Rashid et al. 2018; Sunehag et al. 2017; Yu et al. 2022), including policy gradient-based and value-based ones. The policy-based methods, such as MADDPG(Lowe

et al. 2017), COMA (Foerster et al. 2018b) and MAPPO (Yu et al. 2022) use the information (observations and actions) of the controlled agents to train the team policy. The value-based methods on the other hand, with VDN (Sunehag et al. 2017) and QMIX (Rashid et al. 2018) as the exemplars, construct a joint value function for the controlled agents. These works normally regard the opponents (if exist) as a part of the environment.

However, some people argue that the controlled agent should be endowed with abilities to reason about the opponents’ unknown goals and behaviours to benefit the decision-making, thus coming up with opponent modelling (Albrecht and Stone 2018). By successfully modelling the opponents, the agent can reliably estimate opponents’ behaviours as well as their goals, and adjust its policy to achieve optimal decision-making. Several recent works have proposed learning opponent models using deep learning architectures (He et al. 2016; Foerster et al. 2018a; Raileanu et al. 2018; Tian et al. 2019; Yang et al. 2018).

Nonetheless, the existing works commonly assume access to the opponents’ observations and actions during *both* training and execution. Recent works relax the requirement of access to opponents’ observations and actions during execution (Papoudakis, Christianos, and Albrecht 2021, 2020). However, they still assume the opponents’ information as the ground truth for training the opponent models. We observe that access to the opponents’ real observations and actions during training may not be available or cheap in many cases. For instance, even in a simulator where the user has complete control, the opponent’s policy can come from third-party resources, and thus, its observation format is unknown. When it comes to realistic training environments, although we have the full knowledge of the opponents’ configuration, collecting the opponents’ running data induces high costs as the number of agents and task complexity increase. In these cases, the controlled agent can only rely on its locally available information (i.e., its own observations, actions, and rewards) to model its opponents if it wants to benefit from opponent modelling, which seems counter-intuitive. Thus, a natural but challenging question is: Can we portray the opponents’ behaviours with only the controlled agent’s *local* information?

To answer this question, this work aims to estimate the opponents’ behaviours with *only* the controlled agent’s local

*Corresponding author

information. For this purpose, we design a novel opponent modelling workflow. That is, the controlled agent first speculates its opponents' behaviours using opponent models conditioned on its local information; Then, the controlled agent makes decisions based on its speculation. Due to this design, the agent's decisions are deeply coupled with the opponent models. We expect that a better opponent model can improve the decision quality because it provides the controlled agent with more accurate information about the opponents. Therefore, it is possible to use the return resulting from the controlled agent's decisions as one kind of feedback, which takes the place of the true opponent information, to train the opponent models. This is the key insight of our work.

Following the above workflow, we propose the Distributional Opponent-aided Multi-agent Actor-Critic (DOMAC), an innovative algorithm tailored for speculative opponent modelling utilizing solely local information. The approach consists of two primary modules: the Opponent-aided Actor (OMA) and the Centralized Distributional Critic (CDC). Within the OMA, the controlled agent, i.e., the actor, maintains one opponent model for each opponent, which predicts the opponent's actions based on the controlled agent's local information. Although these inputs are not directly from the opponent strategies, they still correlate with the opponents' behaviours. For example, the opponents could appear in the observations of the controlled agents, thus the local observations can occasionally convey the state-changing information of the opponents. Since our opponent modelling does not use the opponents' information as the ground truth during training or execution, we call our opponent models the *speculative opponent models*. These speculative opponent models are integral to enhancing the actor's decision-making capabilities by providing refined predictions for improved performance. Meanwhile, to gather as much feedback as possible for training the OMA, the CDC capitalizes on the concept of distributional critics (Bellemare, Dabney, and Munos 2017; Dabney et al. 2018a,b; Bellemare, Dabney, and Rowland 2023; Lyu and Amato 2020; Hu et al. 2020; Sun, Lee, and Lee 2021; Huang et al. 2022) to appraise the distribution of the actor's returns, rather than the conventional scalar estimate. This distributional perspective allows for the explicit consideration of correlations between values, thereby capturing more information concerning the return. It avails a more nuanced and informative evaluation of the actor's policy that underpins the refinement of the speculative opponent models essential for the actor's optimization. We highlight the following contributions:

- To the best of our knowledge, we are the first work that studies the opponent modelling with purely local information from the controlled agent.
- In the proposed DOMAC algorithm, we have tailored the designs of OMA and CDC. Besides, we are pioneering the use of distributional critics to guide the training of the opponent models, which can inspire future research.
- Furthermore, we present a formal derivation, grounded in the policy gradient theorem, that guides the joint training of both our agent policy and opponent models, bolstering the theoretical foundation of our DOMAC designs.

- Lastly, we empirically show that DOMAC significantly outperforms existing state-of-the-art methods on several challenging multi-agent tasks, including MPE(Lowe et al. 2017), Pomeranian(Resnick et al. 2018), and StarCraft Multiagent Challenge (SMAC) (Samvelyan et al. 2019). The extensive experiments confirm that our method successfully learns reliable opponent models without using the opponents' true information and achieves better task performance with a faster convergence speed than baselines.

The remainder of this paper is organized as follows. Section briefly reviews the works in multi-agent RL, opponent modelling, and distributional RL. Section introduces the preliminaries of the proposed method. Section elaborates on the detailed designs of the DOMAC. Section provides the evaluation experiments and ablations studies. Finally, Section concludes the paper and presents future works.

Related work

Multi-agent reinforcement learning. In recent years, the developments in multi-agent reinforcement learning (MARL) have led to great progress in creating artificial agents that can efficiently cooperate to solve tasks (Hernandez-Leal, Kartal, and Taylor 2019; Zhang, Yang, and Başar 2021; Gronauer and Diepold 2022). MARL algorithms generally fall into two frameworks: centralized and decentralized learning. Centralized methods (Claus and Boutilier 1998) learn a single policy to produce the joint actions of all agents directly, while decentralized learning (Littman 1994) entails each agent independently optimizing its reward. The framework of centralized training and decentralized execution (CTDE) bridges the gap between the two aforementioned frameworks, which permits the sharing of information during training, while policies are only conditioned on the agents' local observations enabling decentralized execution(Lowe et al. 2017). One category of CTDE algorithm is policy gradient methods, wherein each agent consists of a decentralized actor and a centralized critic, which is optimized by the shared information of the controlled agents(Lowe et al. 2017; Foerster et al. 2018b). The value decomposition method is another category, which represents the joint Q-function as a function of agents' local Q-functions (Sunehag et al. 2017; Rashid et al. 2018; Son et al. 2019; Wang et al. 2020). However, these studies often consider opponents (if exist) as part of the environment, failing to explicitly model the influence of the opponents, which yields sub-optimal learning outcomes.

Opponent modelling. Opponent modelling is a research topic that emerged alongside the game theory (Brown 1951). With the powerful representation capabilities of recent deep learning architectures, opponent modelling has ushered in significant progress (Albrecht and Stone 2018).

Type-based reasoning methods (He et al. 2016; Hong et al. 2018; Raileanu et al. 2018; Albrecht and Stone 2017) assume that the opponent has one of several known types and update the belief using their observations obtained during training. Recursive reasoning methods (Yang et al. 2019; Wen et al. 2019b,a) model the beliefs about the mental states of other agents via deep neural networks. The opponent modelling

with online reasoning refers to the online inference of the opponent’s policy through Bayesian inference and formulating a corresponding response (Zheng et al. 2018; Tian et al. 2019; DiGiovanni and Tewari 2021; Fu et al. 2022). The process of modelling opponents with dynamic strategies involves estimating the opponents’ behaviours and corresponding impacts by using the opponent’s learning (Foerster et al. 2017; Grover et al. 2018; Kim et al. 2021; Liu et al. 2019). The opponent modelling with meta-learning is designed to train against a set of known opponent policies to quickly adapt to unknown opponent policies during the testing (Zintgraf et al. 2021; Wu et al. 2022). Theory of mind-based opponent modelling reasons about opponent’s mental status and intentions, to predict and adapt to opponent behaviour by modelling their beliefs, goals, and actions (Yang et al. 2018; Rabinowitz et al. 2018). However, the aforementioned works commonly assume access to the opponents’ observations and actions during both training and execution. Recent research (Papoudakis, Christianos, and Albrecht 2020, 2021) argues that access to opponents’ observations and actions during execution is often infeasible (e.g., in large-scale applications). They manage to learn an opponent model that only uses the local information of the agent, such as its observations, actions, and rewards during execution. Nevertheless, the efficacy of their methods is constrained by the necessity of accessing opponents’ genuine data during the training phase, a requirement that significantly restricts their applicability in situations where such information is unobservable. Thus, how to model an opponent’s policy when its information is unavailable during training is still an open research problem. Our work presents the first attempt to solve this challenge.

Distributional reinforcement learning. Distributional reinforcement learning (RL) aims to model the return distributions rather than the expected return and uses these distributions to evaluate and optimize a policy (Bellemare, Dabney, and Munos 2017; Dabney et al. 2018a,b; Bellemare, Dabney, and Rowland 2023). Many studies have shown that distribution RL can achieve better performance than the state-of-art methods from the classical RL (Barth-Maron et al. 2018; Tessler, Tennenholz, and Mannor 2019; Singh, Lee, and Chen 2020; Yue, Wang, and Zhou 2020; Bai et al. 2023; Zhang et al. 2023; Wiltzer, Meger, and Bellemare 2022). The Categorical DQN (C51) (Bellemare, Dabney, and Munos 2017) employed a discrete set of N fixed values to approximate the return distribution, achieving superior performance than DQN. Then, Dabney et al. introduced QR-DQN (Dabney et al. 2018b), by appealing to the principle of quantile regression (QR) (Koenker and Hallock 2001), which assigns N fixed and uniform probabilities to adjustable values. Furthermore, an extension to QR-DQN was realized through implicit quantile networks (IQNs) (Dabney et al. 2018a), which learn the entire quantile function via neural networks. Interestingly, the latest research in Nature also shows that similar distributional mechanisms exist in human brains (Dabney et al. 2020), motivating a variety of hybrid methodologies to blend these distributional methods with existing RL techniques to address issues within single-agent (Barth-Maron et al. 2018; Ma et al. 2020) and multi-agent scenarios (Lyu and Amato 2020; Hu et al. 2020; Sun, Lee, and Lee 2021; Huang et al.

2022).

Our work is the first to investigate distributional RL for opponent modelling. Together with previous works, we show the great potential of distributional RL and can attract more research efforts to this area.

Preliminary

Partially observable Markov games. A *partially observable Markov game* (POMG) (Lowe et al. 2017) of n agents is formulated as a tuple $\mathcal{M} = \langle \mathcal{S}, \mathbb{O}, \mathcal{O}, \mathcal{A}, \mathcal{T}, \mathcal{R}, \gamma \rangle$. \mathcal{S} is a set of states describing the possible configuration of all agents and the external environment. Also, each agent i has its own observation space $\mathbb{O}_i \in \mathbb{O}$. Due to the *partial observability*, in every state $s \in \mathcal{S}$, each agent i gets a correlated observation o_i based on its observation function $\mathcal{O}_i : \mathcal{S} \rightarrow \mathbb{O}_i$ where $\mathcal{O}_i \in \mathcal{O}$. The agent i selects an action $a_i \in A_i$ from its own action space $A_i \in \mathcal{A}$ at each time step, giving rise to a joint action $[a_1, \dots, a_n] \in A_1 \times A_2 \times \dots \times A_n$. The joint action then produces the next state by following the state transition function $\mathcal{T} : \mathcal{S} \times A_1 \times \dots \times A_n \rightarrow \mathcal{S}$. $\mathcal{R} = \{r_i\}$ is the set of reward functions. After each transition, agent i receives a new observation and obtains a scalar reward as a function of the state and its action $r_i : \mathcal{S} \times A_i \rightarrow \mathbb{R}$. The initial state $s \in \mathcal{S}$ is determined by some prior distribution $p : \mathcal{S} \rightarrow [0, 1]$. Each agent i aims to maximize its own total expected return $R_i = \mathbb{E}_{r^t \sim r_i(s_t, a_i^t), (s_t, a_i^t) \sim \tau} \sum_{t=0}^T \gamma^t r^t$, where γ is the discount factor, r^t is its sampled reward at time step t , τ is the trajectory distribution induced by the joint policy of all agents, and T is the time horizon. Without loss of generality, we assume that the n agent can be divided into $|M| \leq n$ teams, and each team has q agents with $1 \leq q \leq n$. We consider the teams out of our control as opponent agents with static policies. Note that a single agent can also form a team. We assume agents from the same team fully cooperate and thus share the same reward function.

Actor-Critic method. The actor-critic algorithm (Konda and Tsitsiklis 2000) is a subclass of policy gradient methods (Silver et al. 2014). It has been widely used for tackling complex tasks. The algorithm consists of two components. The *critic* Q_ϕ^π estimates the true action-value function $Q^\pi(s, a)$ that represents the expected return of taking action a in state s and then following policy π . It adjusts the parameters ϕ with an appropriate policy evaluation algorithm such as temporal-difference learning (Sutton and Barto 2018). With the critic, the *actor* adjusts the parameter θ of the agent’s policy π_θ by applying the policy gradient theorem (Sutton et al. 2000):

$$\nabla_\theta J(\theta) = \mathbb{E}_{\pi_\theta} [\nabla_\theta \log \pi_\theta(a|s) Q_\phi^\pi(s, a)]. \quad (1)$$

In multi-agent scenarios, the actor-critic algorithm is applied to learn the optimal policy for each agent. To stabilize the training, it is common to adopt the centralized training and decentralized execution (CTDE) setting (Hernandez-Leal, Kartal, and Taylor 2019), where the agent i ’s action-value function $Q_i^{\pi_i}(\mathbf{o}, \mathbf{a})$ takes as input the joint observation and joint action of the agents in the same controlled team. The gradient of the policy for agent i is given as:

$$\nabla_{\theta_i} J(\theta_i) = \mathbb{E}_{\pi_{\theta_i}} [\nabla_{\theta_i} \log \pi_{\theta_i}(\mathbf{a}|\mathbf{o}) Q_\phi^\pi(\mathbf{o}, \mathbf{a})]. \quad (2)$$

Distributional reinforcement learning. Unlike traditional RL whose target is to maximize the expected total return, distributional RL (Bellemare, Dabney, and Munos 2017) explicitly considers the randomness of the return distribution. The expected discounted return Q^π can be written as:

$$Q^\pi(s, a) = \mathbb{E}[Z^\pi(s, a)] = \mathbb{E}\left[\sum_{t=0}^{\infty} \gamma^t r(s_t, a_t)\right], \quad (3)$$

where $s_t \sim P(\cdot | s_{t-1}, a_{t-1})$, $a_t \sim \pi(\cdot | s_t)$, $s_0 = s$, $a_0 = a$. $Z^\pi(s, a)$ is the return distribution, covering all sources of intrinsic randomness, including reward function, state transition, stochastic policy sampling, and systematic stochasticity. In the distributional RL, we directly model the random return $Z^\pi(s, a)$ instead of its expectation. The distributional Bellman equation can be defined as:

$$Z(s, a) \stackrel{D}{=} r(s, a) + \gamma P^\pi Z(s, a), \quad (4)$$

where $\stackrel{D}{=}$ means the two sides of the equation are distributed according to the same law, $P^\pi Z(s, a) \stackrel{D}{=} Z(S', A')$ and $S' \sim P(\cdot | s, a)$, $A' \sim \pi(\cdot | S')$.

In general, the distribution of the random variable $Z(s, a)$ is represented as $\frac{1}{K} \sum_{j=1}^K \delta_{G_\phi^j(\mathbf{o}, \mathbf{a})}$ where $\delta_{G_\phi^j(\mathbf{o}, \mathbf{a})}$ denotes a Dirac with respect to the support $G_\phi^j(\mathbf{o}, \mathbf{a}) \in \mathbb{R}$. Furthermore, each $G_\phi^j(\mathbf{o}, \mathbf{a})$ can be estimated through optimizing the quantile Huber loss (Dabney et al. 2018a):

$$\mathcal{L}_{QR} = \frac{1}{K^2} \sum_{j'=1}^K \sum_{j=1}^K [\rho_{\omega_j}(\delta_{ij})], \quad (5)$$

where $\rho_{\omega_j}(\mu) = |\omega_j - \mathbb{1}_{\mu \leq 0}| \mathcal{L}_\kappa(\mu)$ and $\delta_{ij} = r + \gamma G_j(\mathbf{o}', \mathbf{a}') - G_j(\mathbf{o}, \mathbf{a})$. $\mathbb{1}_{\mu \leq 0}$ is an indicator function which is 1 when $\mu \leq 0$ and 0 otherwise. κ is a pre-fixed threshold and the Huber loss $\mathcal{L}_\kappa(\mu)$ is given by,

$$\mathcal{L}_\kappa(\mu) = \frac{1}{2} \mu^2 \mathbb{1}_{[|\mu| \leq \kappa]} + \kappa(|\mu| - \frac{1}{2} \kappa) \mathbb{1}_{[|\mu| > \kappa]}. \quad (6)$$

Methodology

The Overall Framework

Our training follows the CTDE setting, i.e., we have the access to the observations and actions of the team we control. Note that, however, we **do not know** the observations and actions of the opponent team during the training. Figure 1 depicts the overall framework of the proposed *distributional opponent model aided actor-critic* (DOMAC) algorithm. We show the meaning of the notifications in Table 1.

Within the DOMAC framework, each controlled agent i incorporates two primary constituents: the Opponent Model Aided Actor (OMA) and the Centralized Distributional Critic (CDC). For p opponents, agent i employs p individualized conjectural opponent models, wherein each model is instantiated as a distinct neural network. These models process the agent's localized observational data and sample actions at each timestamp to ascertain the presumptive action distributions of the opponents. The OMA leverages these models

Table 1: Notations of algorithm

Notation	Meaning
p	The numbers of opponents
$\mu_{\psi_{ik}}$	Predicted opponent model for opponent k of agent i
o_i	Local observation of agent i
\hat{a}_{ik}^t	Predicted opponent actions for opponent k of agent i
π_{θ_i}	Policy network of agent i
a_i^t	Action of agent i
$Z_i(\mathbf{o}^t, \mathbf{a}^t)$	Final agent policy distribution
G_{ϕ_i}	Return distribution of agent i
ω	CDC network
δ_z	Quantiles
K	Dirac at $z \in \mathbb{R}$
α_i	Quantile number
	hyperparameter of exploration

to infer potential joint actions, representing the agent's conjectures concerning the opponents' prospective moves. The agent i 's own action distribution is subsequently determined as a composite function of the outputs from the OMA and the observations, effectively assimilating the agent's tactical considerations with the inferences drawn from the opponent models by performing a weighted aggregation. To enhance predictive precision, the agent samples multiple opponents' joint actions. Intriguingly, the opponent models' training regimen is predicated on the rewards obtained by the agent's policy alone, eschewing reliance on the opponents' genuine actions and underscoring outcome-oriented feedback loops. Meanwhile, the CDC's role is to evaluate the return distribution associated with the agent's policy, preferring a distributional perspective over singular expected value estimations. This methodological choice for estimating returns confers a more nuanced depiction, which polishes the refinement process for the agent's strategic policy.

Note that each agent in the controlled team has an independent set of OMA and CDC, and the only shared are their observations and actions. This is critical for extracting the individual knowledge of each agent, which may be heterogeneous for their different observations, current statuses, etc. To speed up the learning, we share the parameters of the agent networks across all controlled agents but a one-hot encoding of the $agent_id$ is concatenated onto each agent's observations to induce heterogeneities of the inputs. In scenarios where the agents within a system are homogeneous, both functionally and behaviorally, the utilization of a shared OMA network is feasible for these homogeneous agents. Generally, the rationales of DOMAC can be explained as the same closed optimization loop as that of the original actor-critic framework. That is, OMA receives the local information with the beliefs of modelled opponents (i.e., predicted opponents' actions). It improves decision-making quality by adjusting opponent models and actively selecting the actions with higher evaluations according to CDC, while CDC, in turn, evaluates the improved policy. In the following, we first show that optimizing the OMA can be formulated as a policy gradient

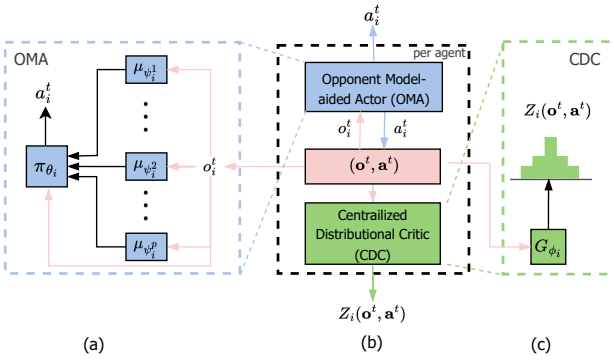


Figure 1: The DOMAC framework. In OMA, the speculative opponent model μ_{ψ_i} takes the local observation o_i^t as input and outputs the prediction of the opponent behaviours. The agent policy network takes action by considering the predicted opponent’s actions. The CDC takes the joint observation \mathbf{o}^t and action \mathbf{a}^t of the controlled agents into the agent critic network G_{ϕ_i} and outputs the return distribution $Z_i(\mathbf{o}^t, \mathbf{a}^t)$.

theorem. Then we formulate the optimization of CDC by using a quantile regression loss. Finally, we transform the theoretical findings into a practical algorithm.

Opponent Model Aided Actor

Suppose the agent i has total p opponents in the game, it represents them by p independent speculative opponent models. Specifically in Figure 2(a), the opponent model for opponent k of agent i is given as $\mu_{\psi_{ik}}$ with trainable parameter ψ_{ik} . Once the agent i receives a local observation o_i^t at time step t , each of its opponent models takes o_i^t and the opponent index k as input, and outputs a distribution over which the opponent k ’s actions \hat{a}_{ik}^t can be predicted.

Then, the agent policy π_{θ_i} takes the joint predicted action $\hat{a}_i^t = [\hat{a}_{i1}^t, \dots, \hat{a}_{ip}^t]$ of all opponents with o_i^t as input, and outputs a distribution over the agent i ’s action space A_i . The final action probability distribution of the agent is the sum of the actor outputs weighted by the probability of corresponding opponent joint action (Equation 7). To increase the accuracy, agent i samples and aggregate multiple opponents’ joint actions.

Then, we connect our OMA module with the Policy Gradient Theorem (Sutton et al. 2000). For clarity, we omit time step t in all formulas below. Let $\mu_{\psi_{ik}}$ and π_{θ_i} be parameterized with the trainable parameters ψ_{ik} and θ_i , respectively, and $\psi_i = \{\psi_{ik}\}$ be the set of parameters of all speculative opponent models maintained by the agent i . We assume that these opponent models are independent with each other. Given an observation o_i , the agent i ’s OMA calculates its action probability distribution as:

$$\begin{aligned} \rho_{\theta_i, \psi_i}(a_i | o_i) &= \sum_{\hat{a}_i} [\pi_{\theta_i}(a_i | \hat{a}_i, o_i) P(\hat{a}_i | o_i)] \\ &= \sum_{\hat{a}_i} [\pi_{\theta_i}(a_i | \hat{a}_i, o_i) \prod_{k=1}^p \mu_{\psi_{ik}}(\hat{a}_{ik} | o_i)], \quad (7) \end{aligned}$$

where $\hat{a}_i = [\hat{a}_{i1}, \dots, \hat{a}_{ip}]$ is an opponent joint action predicted by the agent i ’s opponent models. Then, the objective of agent i is to maximize its total expected return, which is determined by the parameters θ_i and ψ_i :

$$J(\theta_i, \psi_i) = \mathbb{E}_{\mathbf{o} \sim \tau, a_i \sim \rho_{\theta_i, \psi_i}} [\mathbb{E}(Z_i(\mathbf{o}, \mathbf{a}))], \quad (8)$$

where (\mathbf{o}, \mathbf{a}) represents the joint observation and joint action of the agent i ’s team, and τ represents the trajectory distribution induced by all agents’ policies. Additionally, we add the entropy of the policy into the objective function (8) to ensure an adequate exploration, which is proved to be effective for improving the agent performance (Mnih et al. 2016). Thus, the OMA’s final objective can be defined as:

$$J(\theta_i, \psi_i) = \mathbb{E}_{\mathbf{o}, a_i} [\mathbb{E}(Z_i(\mathbf{o}, \mathbf{a})) - \alpha_i \log \rho_{\theta_i, \psi_i}(a_i | o_i)], \quad (9)$$

where α_i is a hyperparameter controlling the degree of exploration. Next, we mathematically derive the closed form of the policy gradient and opponent model gradient respectively, which is summarized in the following proposition.

Theorem 0.1. *In a POMG, under the opponent modelling framework defined, the gradient of parameters θ_i for the policy of the agent i is given as:*

$$\begin{aligned} \nabla_{\theta_i} J(\theta_i, \psi_i) &= \mathbb{E}_{\rho_{\theta_i, \psi_i}} [\nabla_{\theta_i} \log(\rho_{\theta_i, \psi_i}) \cdot \\ &\quad [\mathbb{E}(Z_i) - \alpha_i \log(\rho_{\theta_i, \psi_i}) - \alpha_i]], \end{aligned} \quad (10)$$

and the gradient of the parameters ψ_{ik} for the opponent model $\mu_{\psi_{ik}}$ is given as:

$$\begin{aligned} \nabla_{\psi_{ik}} J(\theta_i, \psi_i) &= \mathbb{E}_{\rho_{\theta_i, \psi_i}} [\nabla_{\psi_{ik}} \log(\rho_{\theta_i, \psi_i}) \cdot \\ &\quad [\mathbb{E}(Z_i) - \alpha_i \log(\rho_{\theta_i, \psi_i}) - \alpha_i]], \end{aligned} \quad (11)$$

where ρ_{θ_i, ψ_i} is defined in Equation (7).

Proof. For notational convenience, $Z_i(\mathbf{o}, \mathbf{a})$ can be considered as Z_i , and $\rho_{\theta_i, \psi_i}(a_i | o_i)$ can be simplified as ρ_{θ_i, ψ_i} . Then the objective in Equation (6) can be written as:

$$J(\theta_i, \psi_i) = \sum_{a_i} \rho_{\theta_i, \psi_i} [\mathbb{E}(Z_i) - \alpha_i \log \rho_{\theta_i, \psi_i}]. \quad (12)$$

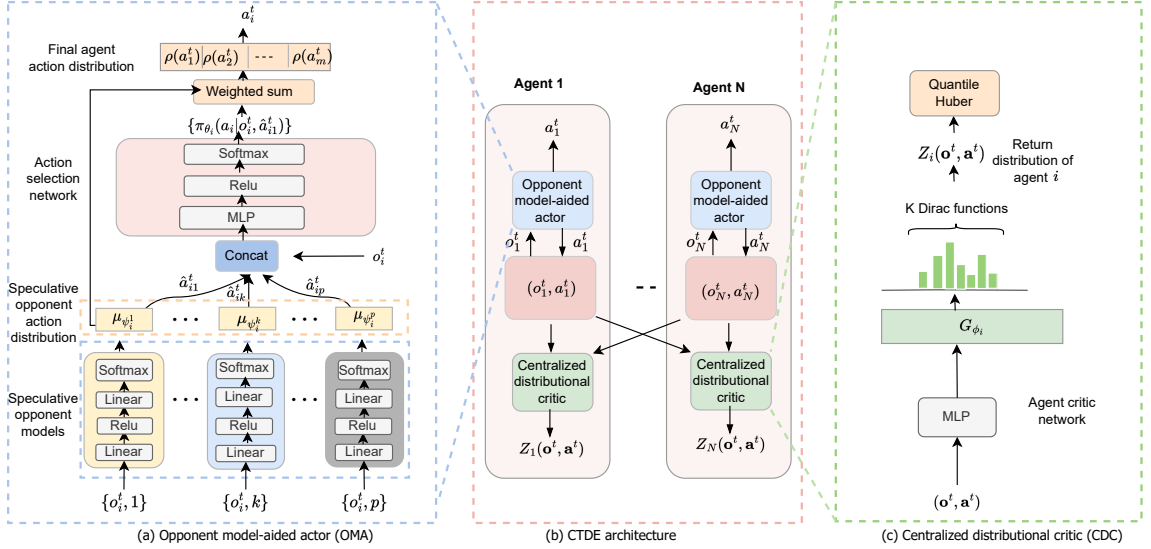


Figure 2: An illustration of our DOMAC network architecture. (a) Opponent model-aided actor: Each model contains p speculative opponent models, which take the local observation o_i^t and opponent index k as inputs to predict the opponents' actions. Then, the action selection network π_{θ_i} takes the joint predicted action $\{\hat{a}_i^t\}$ together with the o_i^t and a_i^{t-1} as input, and outputs a distribution over the agent i 's own actions, which is weighed according to the probabilities of predicted opponents' actions $\mu_{\phi_i}^k$ for $1 \leq k \leq p$. (b) CTDE architecture: we have the access to the observations and actions of the team we control. (c) Centralized distributional critic: the agent critic network takes the joint observation \mathbf{o}^t and action \mathbf{a}^t of the controlled agents and outputs G_{ϕ_i} as the approximation of return distribution.

The policy gradient of parameter θ_i can be calculated as:

$$\begin{aligned}
 \nabla_{\theta_i} J(\theta_i, \psi_i) &= \sum_{a_i} \nabla_{\theta_i} \rho_{\theta_i, \psi_i} \mathbb{E}(Z_i) \\
 &\quad - \alpha_i \sum_{a_i} \nabla_{\theta_i} [\rho_{\theta_i, \psi_i} \log \rho_{\theta_i, \psi_i}] \\
 &= \sum_{a_i} \nabla_{\theta_i} \rho_{\theta_i, \psi_i} \mathbb{E}(Z_i) \\
 &\quad - \alpha_i \sum_{a_i} \nabla_{\theta_i} \rho_{\theta_i, \psi_i} [\log \rho_{\theta_i, \psi_i} + 1] \\
 &= \sum_{a_i} \nabla_{\theta_i} \rho_{\theta_i, \psi_i} [\mathbb{E}(Z_i) - \alpha_i \log \rho_{\theta_i, \psi_i} - \alpha_i] \\
 &= \sum_{a_i} \rho_{\theta_i, \psi_i} \nabla_{\theta_i} \log \rho_{\theta_i, \psi_i} [\mathbb{E}(Z_i) \\
 &\quad - \alpha_i \log \rho_{\theta_i, \psi_i} - \alpha_i] \\
 &= \mathbb{E}_{\rho_{\theta_i, \psi_i}} \left[\nabla_{\theta_i} \log \rho_{\theta_i, \psi_i} [\mathbb{E}(Z_i) \right. \\
 &\quad \left. - \alpha_i \log \rho_{\theta_i, \psi_i} - \alpha_i] \right].
 \end{aligned} \tag{13}$$

Since $\psi_i = \{\psi_{ik}\}$, then $\nabla_{\psi_i} J(\theta_i, \psi_i) = \{\nabla_{\psi_{ik}} J(\theta_i, \psi_i)\}$. For each opponent agent k , the gradient of parameter ψ_{ik} can be calculated as:

$$\begin{aligned}
 \nabla_{\psi_{ik}} J(\theta_i, \psi_i) &= \sum_{a_i} \nabla_{\psi_{ik}} \rho_{\theta_i, \psi_i} \mathbb{E}(Z_i) \\
 &\quad - \alpha_i \sum_{a_i} \nabla_{\psi_{ik}} [\rho_{\theta_i, \psi_i} \log \rho_{\theta_i, \psi_i}].
 \end{aligned} \tag{14}$$

Based on the Equation (4), we can conclude that the parameters of θ_i and ψ_{ik} are independent. Then we can further obtain that

$$\begin{aligned}
 \nabla_{\psi_{ik}} J(\theta_i, \psi_i) &= \mathbb{E}_{\rho_{\theta_i, \psi_i}} \left[\nabla_{\psi_{ik}} \log \rho_{\theta_i, \psi_i} [\mathbb{E}(Z_i) \right. \\
 &\quad \left. - \alpha_i \log \rho_{\theta_i, \psi_i} - \alpha_i] \right].
 \end{aligned} \tag{15}$$

Note that ρ_{θ_i, ψ_i} conditions on ψ_{ik} as shown in Equation (7). Therefore, the operation $\nabla_{\psi_{ik}} \log(\rho_{\theta_i, \psi_i})$ in Equation (11) enables the gradients to naturally backpropagate to the opponent models. This proposition states that OMA can adjust the parameters θ_i and ψ_i towards maximizing the objective by following the gradient. Intuitively speaking, the OMA directly searches the optimal policy and reliable opponent models by looking at the agent's objective, which does not require access to opponents' true information. Although it may look weak to use the objective as the only learning signal, we will show that the gradient of the objective is already sufficient for training reliable opponent models and thereby good actors.

Centralized Distributional Critic

To enhance training and provide a more delicate evaluation of the OMA, we adopt a distributional perspective to evaluate agents' performance by modelling their return distributions (Bellemare, Dabney, and Munos 2017). We propose to learn a centralized distributional critic (CDC) for each controlled agent i . After all agents in the controlled team sample their actions, each controlled agent i 's CDC network G_{ϕ_i} takes as input the joint observation \mathbf{o}^t and joint action \mathbf{a}^t of its

team, and computes a return distribution $Z_i(\mathbf{o}^t, \mathbf{a}^t)$. Following (Dabney et al. 2018b), we train the CDC with the quantile regression technique. Specifically, we implement the CDC for the agent i as a deep neural network G_{ϕ_i} with ϕ_i being the trainable parameters. Given the joint observation and joint action (\mathbf{o}, \mathbf{a}) of the agent i 's team, G_{ϕ_i} outputs a K -dimensional vector $\{G_{\phi_i}^j(\mathbf{o}, \mathbf{a})\}_{j=1, \dots, K}$. The elements of this output are the samples that approximate the agent i 's return distribution $Z_i(\mathbf{o}, \mathbf{a})$. That is, we can represent the distribution approximation as $\frac{1}{K} \sum_{j=1}^K \delta_{G_{\phi_i}^j(\mathbf{o}, \mathbf{a})}$ where δ_z denotes a Dirac at $z \in \mathbb{R}$. An ideal approximation can map these K samples to K fixed quantiles $\{\omega_j = \frac{j}{K}\}_{j=1, \dots, K}$ so that $P(Z_i(\mathbf{o}, \mathbf{a}) \leq G_{\phi_i}^j(\mathbf{o}, \mathbf{a})) = \omega_j$. To approach that, we compute the target distribution approximation $\hat{G}_{\phi_i}(\mathbf{o}, \mathbf{a})$ based on the distributional Bellman operator,

$$\hat{G}_{\phi_i}(\mathbf{o}, \mathbf{a}) = \{r(s, \mathbf{a}) + \gamma G_{\phi_i}^j(\mathbf{o}', \mathbf{a}')\}_{j=1, \dots, K}, \quad (16)$$

where $\mathbf{o}' \sim \tau$, $\mathbf{a}' = \arg \max_{\mathbf{a}'} \mathbb{E}[G_{\phi_i}(\mathbf{o}', \mathbf{a}')]$. The objective of the CDC training then becomes minimizing the distance between \hat{G}_{ϕ_i} and G_{ϕ_i} . To this end, we use the Quantile Huber loss (Dabney et al. 2018b),

$$\mathcal{L}_{QR} = \frac{1}{K^2} \sum_{j'=1}^K \sum_{j=1}^K [\rho_{\omega_j}(\hat{G}_{\phi_i}^{j'}(\mathbf{o}, \mathbf{a}) - G_{\phi_i}^j(\mathbf{o}, \mathbf{a}))], \quad (17)$$

where $\rho_{\omega_j}(\mu) = |\omega_j - \mathbb{1}_{\mu \leq 0}| \mathcal{L}_\kappa(\mu)$. $\mathbb{1}_{\mu \leq 0}$ is an indicator function which is 1 when $\mu \leq 0$ and 0 otherwise. κ is a pre-fixed threshold and the Huber loss $\mathcal{L}_\kappa(\mu)$ is given by,

$$\mathcal{L}_\kappa(\mu) = \frac{1}{2} \mu^2 \mathbb{1}_{[|\mu| \leq \kappa]} + \kappa(|\mu| - \frac{1}{2} \kappa) \mathbb{1}_{[|\mu| > \kappa]}. \quad (18)$$

Practical Algorithm

We now present a tangible algorithm for training OMA and CDC. First, we describe a sampling trick that is essential for training. For OMA, the controlled agent maintains a set of opponent models, each of which is instantiated by an independent neural network and corresponds to an opponent. Thus, the number of opponent models and overall network size is linear with the number of opponents, which can be easily handled by GPU parallel training. However, computing the marginal distribution ρ_{θ_i, ψ_i} can be exponentially costly concerning the dimensionality of the opponents' action space according to Equation (7). Formally, each agent i 's opponent k has $|A_{ik}|$ actions. Then calculating the exact ρ_{θ_i, ψ_i} requires traversing $|A_{i1}| \times \dots \times |A_{ip}|$ opponent joint actions, which quickly becomes intractable as p increases. To address this issue, in our algorithm, we apply a sampling trick that samples a set of actions $\hat{a}_{ik} = (\hat{a}_{ik1}, \dots, \hat{a}_{ikl})$ from the output of the speculative opponent model $\mu_{\psi_{ik}}$ for each opponent k , where l controls the size of sampled actions. Then, $\rho_{\theta_i, \psi_i}(a_i | o_i)$ can be approximated as:

$$\bar{\rho}_{\theta_i, \psi_i}(a_i | o_i) = \sum_l \pi_{\theta_i}(a_i | o_i, \{\hat{a}_{ikl}\}) \prod_{k=1}^p \mu_{\psi_{ik}}(\hat{a}_{ikl} | o_i).$$

The action a_i can be sampled from $\bar{\rho}_{\theta_i, \psi_i}(a_i | o_i)$ for each agent i . We use empirical samples $\{G_{\phi_i}^j(\mathbf{o}, \mathbf{a})\}_{j=1, \dots, K}$ to

Algorithm 1: Training Procedure of DOMAC

Require: A POMG environment env , a back-propagation optimizer Opt , number of episodes E , number of forward steps T_f , and π_{θ_i} , μ_{ψ_i} , G_{ϕ_i} with initialized parameters θ_i , ψ_i , and ϕ_i for each agent i .

```

1: for  $e = 1, \dots, E$  do
2:    $t \leftarrow 1$ ; Reset  $env$  to obtain initial observations  $\mathbf{o}^1$ 
3:   while  $env$  is not done do // Generate data
4:     for  $t^* = t, \dots, t + T_f - 1$  do
5:       Sample each agent  $i$ 's action  $a_i^{t^*} \sim \rho_{\theta_i, \psi_i}(a_i^{t^*} | o_i^{t^*})$ 
6:       Form the controlled team's joint action  $\mathbf{a}^{t^*} = \{a_i^{t^*}\}$ 
7:       Execute  $\mathbf{a}^{t^*}$  to obtain  $\mathbf{r}^{t^*}$  and  $\mathbf{o}^{t^*+1}$ 
8:       Store transition data  $(\mathbf{o}^{t^*}, \mathbf{a}^{t^*}, \mathbf{r}^{t^*}, \mathbf{o}^{t^*+1})$ 
9:     end for
10:    for  $1 \leq i \leq n$  do // Update OMA, CDC
11:      Calculate  $Z_i, \bar{\rho}_{\theta_i, \psi_i}$  with collected data
12:      Updates  $G_{\phi_i}$  by minimizing Equation (5)
13:      Updates  $\pi_{\theta_i}$  by minimizing Equation (19)
14:      Updates  $\mu_{\psi_i}$  by minimizing Equation (19)
15:    end for
16:     $t \leftarrow t + T_f$ 
17:  end while
18: end for

```

approximate $Z_i(\mathbf{o}, \mathbf{a})$. The objective function of OMA is,

$$J(\theta_i, \psi_i) = \mathbb{E}_{\mathbf{o}, a_i} \left[\frac{1}{K} \sum_{j=1}^K G_{\phi_i}^j(\mathbf{o}, \mathbf{a}) - \alpha_i \cdot \log \bar{\rho}_{\theta_i, \psi_i}(a_i | o_i) \right]. \quad (19)$$

We incorporate the proposed OMA and CDC into the on-policy framework. In general, the training procedure of DOMAC is similar to that of other on-policy multi-agent actor-critic algorithms (Foerster et al. 2018b), where the training data is generated on the fly. At each training iteration, the algorithm first generates training data with the current OMA and CDC. Then, we compute the objectives of OMA and CDC from the generated data, respectively. At last, the optimizer updates the parameters ϕ_i , θ_i , and ψ_i accordingly. After that, the updated OMA and CDC are used in the next training iteration. In practice, we can parallelize the training, which is a common technique to reduce the training time (Iqbal and Sha 2019). In such cases, the training data is collected from all parallel environments, and actions are sampled and executed in respective environments concurrently. We summarize the training procedure in Algorithm 1.

Experiments

To thoroughly assess the DOMAC algorithm, we evaluate our model in three widely-used partial observable multi-agent environments for various settings. The environments are the predator-prey game based on the Multi-agent Particle Environment (Lowe et al. 2017), the Pommerman Environment (Resnick et al. 2018) and the StarCraft Multiagent Challenge (SMAC) suit (Samvelyan et al. 2019). From the experiments, we aim to answer the following questions: (1): Does the DOMAC yield superior performance than SOTA baseline methods (Figure 5, 6 and Table 2)? (2): Are the main components of DOMAC, i.e., the OMA and CDC, necessary and

effective (Figure 7, Figure 8, Figure 9, and Figure 12)? (3): How do the key hyperparameters in DOMAC affect the final results (Figure 10, Figure 11 and Table 3)?

The Environment Setup

Setup for the predator-prey environment.

In the predator-prey environment (Figure 3(a)), the player controls multiple cooperating predators to catch faster-moving preys in 500 iterations. Every prey has a health of 10. A predator moving within a given range of the prey lowers the prey’s health by 1 point per time step. Lowering the prey’s health to 0 can kill the prey. If there is at least one prey surviving after 500 iterations, the prey team wins. All agents choose among five moving actions. L landmarks (gray circles) that impede the agents’ way are randomly placed in the environment at the start of the game. Each predator obtains the relative positions and velocities of the agents, and the positions of the landmarks as an observation. We evaluate DOMAC in two scenarios. In one scenario, there exist three predators and one prey and we denote it as PP-3v1. Another one includes five predators and two preys and we denote it as PP-5v2. The number of landmarks is 2 in both settings.

Setup for the pommerman environment.

This environment involves four agents. In every step, these agents can move in one of four directions, place a bomb, or do nothing. As shown in Figure 3(b), agents get local observations within their field of view 5×5 , which contains information (board, position, ammo) about the map. An empty grid allows any agents to enter it. A wooden grid cannot be entered but can be destroyed by a bomb. A rigid grid is unbreakable and impassable. When a bomb is placed in a grid, it will explode after 10 time steps. The explosion will destroy any wooden grids and agents which locate within 4-grids away from the bomb. If all agents of one team die, the team loses the game. The game will be terminated after 1000 steps no matter whether there is a winning team or not. Agents get +1 reward if their team wins and -1 reward otherwise. The details of the environments are provided in the supplementary material. We carry out the experiments in two different settings. In the first setting, four agents fight against each other, denoted as Pomm-FFA. The second setting is a two-team competition where each team has two agents, denoted as Pomm-Team.

Setup for StarCraft environments

For the SMAC benchmark (Samvelyan et al. 2019), we adopt the v4.10 StarCraft II simulator. In SMAC, each agent is represented by a troop unit with different attacking abilities. The agents can move in four directions and are allowed to perform the attack action only if the enemy is within its shooting range. As depicted in Figure 4, each agent obtains local observations within its visual radius, capturing details like distance, relative location, health, shield, and unit type for all units (friendly and hostile) within a defined circular sector of the map. At each time step t , each agent receives the same joint reward equal to the cumulative damage dealt to the enemy team until t . In addition, all agents receive a bonus of 10 points after an opponent is killed and 200 points after wiping all enemy team. In addition, these rewards are all normalized to ensure the maximum cumulative reward achievable in an

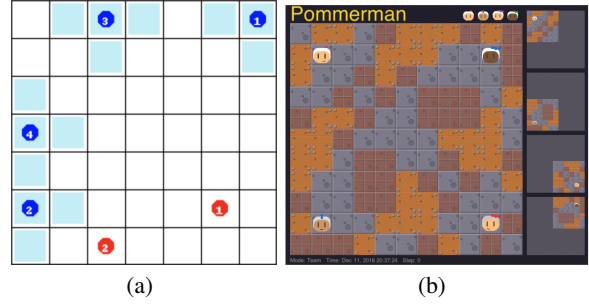


Figure 3: **State visualization of benchmark environments.** (a) The state of a PP-3v1 game, where blue vertices and red vertices denote the predators and prey respectively. (b) The image-based state for the pommerman environment.



Figure 4: **State visualization of StarCraft II,** (a) The state of a MMM2 game, (b) The state of a 5m_vs_6m game.

episode is 20 points. We evaluate our method in four widely-used scenarios: 2s3z (easy and symmetric heterogeneous), 1c3s5z (easy and symmetric heterogeneous), 5m_vs_6m (hard and asymmetric homogeneous), and MMM2 (super hard and symmetric heterogeneous). We provide the details of the three environments in Appendix .

Baselines and Algorithm Configuration.

Baselines.

To the best of our knowledge, this is the first work that considers the opponent modelling problem with purely local information. Because the existing works on opponent modelling all require access to opponents’ true information, they cannot work in our setting. Therefore, we compare the proposed DOMAC algorithm with one of the most popular multi-agent RL algorithms: multi-agent actor-critic (MAAC) (Lowe et al. 2017) which is the discrete version of multi-agent deep deterministic policy gradient (MADDPG). Because MAAC does not incorporate opponent modelling, it is compatible with our setting where opponents’ true information is not available. Also, we further integrate MAAC with our OMA and CDC respectively to generate another two baselines. Let OMAC denote the baseline that combines MAAC with OMA and DMAC denote the baseline that combines MAAC with CDC. The comparison with OMAC and DMAC can demonstrate the impact of OMA and CDC, and thereby justify our design. To comprehensively verify the performance of DOMAC, we also compare it with a state-of-the-art (SOTA) policy gra-

dient algorithm, MAPPO, which has achieved satisfactory performance in many environments (Yu et al. 2022). Furthermore, we evaluate an upper bound setting (denoted as UB) where we directly use the actual opponent policy to predict the opponents’ actions during training. Because the actual opponent policy can provide accurate opponent information to the agent actors, which is the learning goal of our speculative opponent models, the performance of UB can be regarded as the upper bound of the performance of DOMAC.

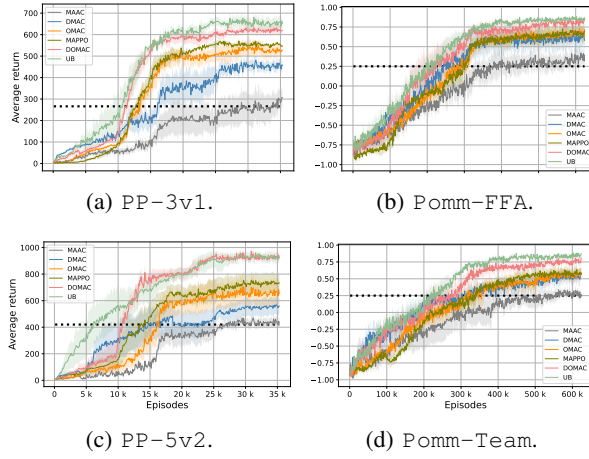


Figure 5: Performance of DOMAC and baselines in the Predator-prey and Pommerman environments.

Algorithm configuration.

For PP-3v1 and PP-5v2, the ρ_{θ_i, ψ_i} and G_{ϕ_i} of each controlled agent i are both multi-layer perceptrons (MLP) with 3 hidden layers of dimensionality 64. We train the networks for $T = 35,600$ episodes using a single environment. The parameters of the networks are updated by Adam optimizer (Kingma and Ba 2015) with learning rate for ρ_{θ_i, ψ_i} and G_{ϕ_i} as $2.5e - 4$ and $1e - 4$. Rather than updating the networks for every T_f steps, we update the networks with data collected from entire 10 episodes because the predator-prey environment consumes less memory for storing data. We set the number of quantiles as $K = 5$, the discounting factor as $\gamma = 0.95$, and the entropy coefficient as $\alpha_i = 0.01$. We have conducted a study on the impact of sample size l . We observe that when l is small, increasing it improves the performance obviously. However, a large sample size only brings marginal benefits while requiring too much computation. Therefore, we set the sample size of PP-5v2 as $l = 10$. The others follow the default setting of Pytorch (Paszke et al. 2017).

The configuration for Pomm-FFA and Pomm-Team is generally the same as that of the predator-prey games. However, here ρ_{θ_i, ψ_i} and G_{ϕ_i} are both convolutional neural networks (CNN) with 4 hidden layers, each of which has 64 filters of size 3×3 , as the observations are image-based. Between any two consecutive CNN layers, there is a two-layer MLP of dimension 128. The learning rate for ρ_{θ_i, ψ_i} and G_{ϕ_i} are both $2.5e - 5$. We parallel 16 environments during training and the number of forward step is $T_f = 5$, that is, we update the networks after collecting 5 steps of data from 16 environments at each iteration. The total number of training episodes is $T = 624,000$. We set the sample size l in

Pomm-FFA and Pomm-Team as 80 and 25 separately.

For environments in SMAC, ρ_{θ_i, ψ_i} and G_{ϕ_i} are both MLP of three hidden layers with dimension 128. The discount factor γ is set to 0.99. The target networks are updated at a frequency of every 100 episodes. The learning rate for ρ_{θ_i, ψ_i} and G_{ϕ_i} are both $5e - 4$. The training steps of 5m_vs_6m and 2s3z are $T = 150,000$, while for mmm2 and 1c3s5z it extends to $T = 2,000,000$. Periodic evaluations are conducted every 10,000 step to assess the models’ performance. Episodes are finished upon the defeat of an entire army or upon reaching a designated time limit. We set the sample size as $l = 323$ for 5m_vs_6m and 2s3z and set $l = 500$ in mmm2 and 1c3s5z. All experiments are carried out in a machine with Intel Core i9-10940X CPU and a single Nvidia GeForce 2080Ti GPU.

Experiment Results

Comparison with Baseline Methods The performance of DOMAC and baseline methods is evaluated based on two criteria: the average return, indicating effectiveness, and the learning speed, reflecting the rate at which proficiency is attained by each method.

Analysis of the average return.

We first compare the overall performance of DOMAC with baselines. The results are summarized in Figure 5 and Figure 6. For the Predator-prey and Pommerman environments, we report the average returns for 8 random seeds. For SMAC, we report the average win rate. Specifically, for PP-3v1 and PP-5v2, we evaluate all the methods with 100 test episodes after every 100 iterations of training, and report the mean (solid lines) and the standard deviation (shaded areas) of the average returns over eight seeds. Similarly, for Pomm-FFA and Pomm-Team, all methods are evaluated with 200 test episodes after every 1,000 training iteration. For the scenarios of SMAC, the methods are evaluated with 32 test episodes after every 5,000 training steps. We report the mean test win rate (percentage of episodes won by controlled team) along with one standard deviation of the test win rate (shaded areas in figures).

From the curves, it is evident that DOMAC’s performance closely aligns with the upper bound while it consistently surpasses the other four benchmarks, achieving faster convergence and demonstrating lower variability in all tested games. This reinforces the effectiveness of DOMAC in forming dependable speculative opponent models without relying on access to actual opponent information. The success of OMAC highlights the benefits of integrating opponent models into the actor-critic framework augmented with a conventional centralized critic, akin to MAAC. Additionally, the superior performance of DMAC over MAAC underscores the value of converting a standard critic into a distributional one, which in turn facilitates the development of more robust policies. These findings individually point to the merits of both Opponent Modelling Advantage (OMA) and Centralized Distributional Critic (CDC) in enhancing performance. Furthermore, when compared to MAPPO (Yu et al. 2022), a state-of-the-art policy gradient algorithm, DOMAC outshines in both sample efficiency and overall performance. This suggests that learning distinct return distributions and accurately anticipating

the actions of unknown opponents can indeed significantly elevate performance.

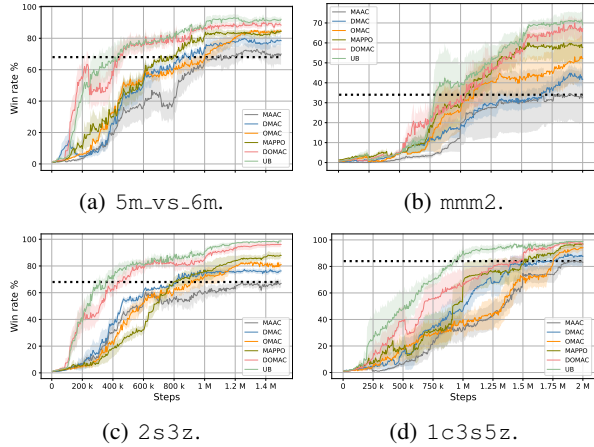


Figure 6: Performance of DOMAC and baseline in the four evaluation scenarios of SMAC.

Analysis of the learning speed.

To demonstrate the efficiency of our approach, we compare the relative learning speed of our methods and baselines with that of MAAC (without loss of generality). This evaluation is defined by the formula $LS = E_{P_{MA}}/T$, where P_{MA} represents the optimal performance for MAAC (indicated by the black dashed line in Figures 5 and 6), and $E_{P_{MA}}$ denotes the episode count at which different methods reach this benchmark performance (including MAAC, DMAC, OMAC, MAPPO, DOAMC, and UB). To give an example, in the scenario PP5v2, with a total of $T = 356000$ training episodes, DOMAC achieves the same performance as P_{MA} at episode 107500, resulting in a relative learning speed of 30.2%. As summarized in Table 2, the learning speed of DOMAC consistently surpasses all other methods by a large margin over all the tested scenarios. Furthermore, it is worth noting that DOMAC exhibits a convergence speed comparable to UB (the baseline trained with ground-truth opponents’ information). The exceptional data efficiency of DOMAC can be attributed to the distributional critic’s role in effectively guiding the opponent modelling process. Meanwhile, the opponent model, in turn, aids the agent’s policy in making more informed decisions. In contrast, DMAC and OMAC are inferior due to the lack of guidance from the opponent models and the distributional critic, respectively.

Table 2: The learning speed of different methods.

	MAAC	DMAC	OMAC	MAPPO	DOMAC	UB
PP3v1	77.4%	36.7%	45.2%	35.3%	31.1%	29.9%
PP5v2	77.1%	42.4%	45.2%	39.5%	30.2%	16.9%
FFA	76.4%	48.1%	52.4%	41.8%	39.1%	35.8%
Team	59.1%	38.5%	42.6%	37.9%	34.5%	32.1%
5m_vs_6m	72.0%	56.3%	66.3%	47.3%	29.3%	27.6%
2s3z	82.7%	54.1%	53.5%	35.3%	31.6%	28.4%
mmm2	88%	82%	55%	53%	51.5%	39.4%
1c3s5z	90%	80.5%	87.5%	75.2%	70.1%	46.7%

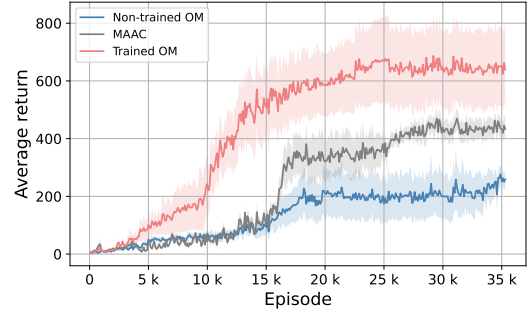


Figure 7: Impacts of the OMA for game PP-5v2.

Ablation studies The ablation studies serve to answer the following questions: (a) Does the OMA and CDC help to learn a better policy? (b) How do the hyperparameters in DOMAC affect the final results?

Ablation studies for OMA. We first verify that the speculative opponent models truly help to learn a better policy. We perform a pair of experiments: the first one uses trained and fixed opponent models and trains the actor from scratch while the second one uses randomly initialized and fixed opponent models instead. The average returns are plotted in Figure 7. It is obvious that the DOMAC with trained opponent models learns faster than the one without, which indicates that the agent can infer the behaviours of its opponents and take advantage of this knowledge to make better decisions, especially at the beginning stage of the learning procedure. It shows that our opponent models can provide reliable information for better decision-making.

While the previous results show that our opponent models improve the decision-making quality, one may wonder whether the improvement really results from the opponent action prediction output by the opponent models. Is it possible that the actor can always get the improvement by conditioning on arbitrary information output by the opponent models? To investigate this question, we change the output dimension d of opponent models to 3, 8, and 16 respectively while retaining the other configurations. We denote these setting as “3AS”, “8AS”, and “16AS” in Figure 8(a). Note that the opponent action space size is 5. Therefore, the opponent models in the three new settings output some conditional information instead of opponent action predictions. The training results over 8 random seeds are shown in Figure 8(a). We can see that the original DOMAC learns faster and better than the other ones. We also notice that the performance of $d = 3$ and $d = 8$ are consistently better than that of $d = 16$ for the entire training period. It implies that the opponent model can infer more reliable information if its output dimension is close to the opponent action space size.

Given the above results, the following question is that why the opponent models perform the best when their architectures are designed to output opponent action prediction. A possible reason is that the opponents sometimes appear in the observations of the controlled agents and thus, the local observations can occasionally convey the state-changing information of the opponents. In this case, the opponent models that output opponent action prediction can indeed learn

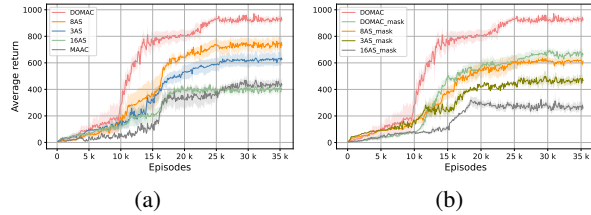


Figure 8: (a) Study of OMA action space in PP-5v2 , (b) Study of masked observation in PP-5v2.

better from the received observations. To verify this hypothesis, we conduct another experiment where we mask out the opponent information when the agent observes the opponents and retains the other configurations. The results are denoted as “X_mask” where “X” means the original algorithm setting. Figure 8(b) shows that when masking out the opponent information, the performance of all algorithms declines, “DOMAC_mask” is weak to “DOMAC”, which means that the opponent model learning indeed benefits from the information contained in the local observations.

To further illustrate that the opponent models can learn reliable opponent behaviours using the local information, we compare our method with the upper bound that directly uses the ground-truth opponent information to infer the opponent’s behaviours. We use game PP-5v2 and Pomm-FFA as the test beds. The results over eight random seeds are shown in Figure 9. Specifically, we perform a pair of experiments, where the first one uses the real opponent observation to infer the opponent’s behaviours, while the second one uses randomly generated information to estimate the opponent’s behaviours. We measure the performance of different settings by computing the distance with the actual opponent’s behaviours. In Figure 9, it is obvious that the DOMAC with local information has a similar performance to the one with true information and significantly outperforms the one with randomly generated information. These results show that our opponent models can effectively reason about the opponents’ intentions and behaviours even with local information.

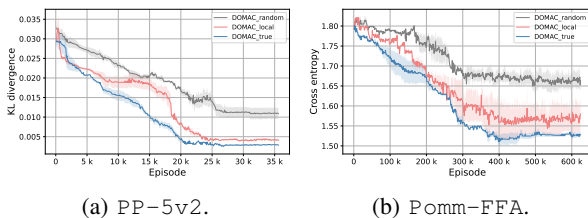


Figure 9: Study of the influence of the local information.

Here we conduct another experiment to examine the impact of sampling size l . We take Pomm-FFA as a demonstration. Given that there are three opponents in FFA and the size of the action space is 6, the size of the joint opponent action space is 216. We consider the sampling size l to be 60, 80, 120, and 180, respectively and keep the rest of the configurations fixed. In Figure 10, we observe that the performance gradually improves with the sampling size. The

performance of $l = 80$ is comparable to that of $l = 120, 180$. We also report the inference time of DOMAC under different sampling sizes. Specifically, $T_{30} = 1.38s$, $T_{60} = 6.1s$, $T_{80} = 9.3s$, $T_{120} = 19.7s$ and $T_{180} = 42.1s$. Therefore, we can conclude that a sample size larger than 100 only brings marginal benefits while costing too much computation. To balance efficiency and performance, we choose $l = 80$ in our experiment.

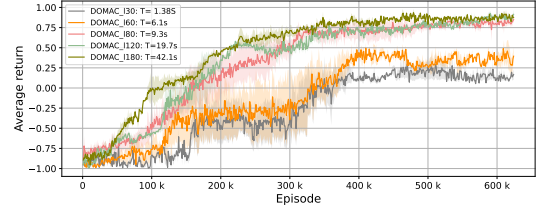


Figure 10: The study of the sample size.

Ablation studies for CDC.

In CDC, we use the quantile representation technique to approximate the return distribution. The number of quantiles may influence the algorithm’s performance. We conduct an ablation study for different values of K under different scenarios to further reveal the influence of the quantile number K during training. We variate the quantile number K to 3, 5, 10, and 15 respectively while fixing other configurations. Here, we present the training curves of our method for games PP-5v2 and 2s3z (Figure 11). We can see that the performance of $K = 5, 10, 15$ quantiles is consistently better than that of $K = 3$ quantiles. This is aligned with the intuition that more quantiles can support more fine-grained distribution modelling. Thus, it better captures the return randomness and improves performance. The results for the rest scenarios are in the appendix (Figure A1). For testing, we summarize the results of the total eight scenarios in Table 3. We show the average return and running time over eight seeds. In the Predator-prey and Pommerman environments, the data was gathered by averaging the returns and calculating the evaluation times at the checkpoint, which achieved the highest average performance during training. In the scenarios of SMAC, we report the median of the final ten evaluation win rates and evaluation times(Wang et al. 2021). The results show that the performance improved with the increase of the quantile number. Nevertheless, it is noteworthy that the computational time exhibits an increasing trend as the number of quantiles expands. To balance computational overhead and performance, we set $K = 5$ throughout the experiments.

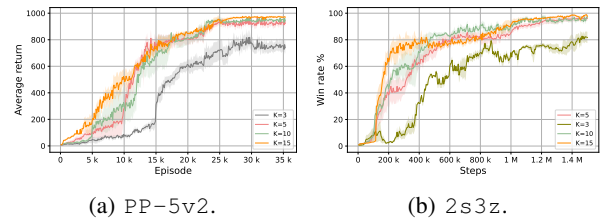


Figure 11: Study of the impact of the quantile numbers.

Table 3: The average evaluation results and running time for different methods on various quantile numbers

Env	K=3		K=5		K=10		K=15	
	Return	Time	Return	Time	Return	Time	Return	Time
PP3v1	651.1 \pm 13.6	4.7 \pm 1.3(s)	708.1 \pm 28.9	8.4 \pm 1.1(s)	816.1 \pm 16.1	21.2 \pm 2.5(s)	754.8 \pm 36.1	41.15 \pm 8.1(s)
PP5v2	857.3 \pm 15.2	6.4 \pm 0.9(s)	938.4 \pm 32.9	13.7 \pm 1.2(s)	969.1 \pm 26.1	23.4 \pm 3.0(s)	974.8 \pm 31.1	44.31 \pm 2.7(s)
FFA	0.783 \pm 0.6	7.2 \pm 2.1(s)	0.842 \pm 0.37	10.5 \pm 1.5(s)	0.871 \pm 0.3	26.1 \pm 2.3(s)	0.91 \pm 0.3	42.8 \pm 8.1(s)
Team	0.817 \pm 0.35	10.1 \pm 2.4(s)	0.871 \pm 0.41	18.1 \pm 1.9(s)	0.886 \pm 0.12	35.8 \pm 3.7(s)	0.94 \pm 0.23	55.1 \pm 6.3(s)
5m_vs_6m	98.3 \pm 0.1%	7.8 \pm 1.4(s)	99.1 \pm 0.01%	15.2 \pm 2.5(s)	99.3 \pm 0.01%	30.77 \pm 4.3(s)	99.8 \pm 0.01%	48.01 \pm 8.8(s)
2s3z	96.1 \pm 0.5%	8.1 \pm 1.3(s)	98.2 \pm 0.06%	14.8 \pm 1.1(s)	98.9 \pm 0.8%	31.25 \pm 2.1(s)	99.1 \pm 0.01%	40.28 \pm 10.2(s)
mmmm2	53.1 \pm 1.6%	13.7 \pm 2.1(s)	60.1 \pm 3.2%	20.7 \pm 4.7(s)	63.4 \pm 2.5%	35.27 \pm 3.8(s)	68.8 \pm 4.3%	44.01 \pm 7.3(s)
1c3s5z	93.1 \pm 1.1%	7.2 \pm 2.5(s)	96.9 \pm 0.1%	19.8 \pm 1.1(s)	97.1 \pm 0.5%	30.13 \pm 3.2(s)	97.3 \pm 0.1%	45.29 \pm 12.1(s)

Exposing connections between OMA and CDC We are curious about how the centralized distributional critic (CDC) impacts the learning of the opponent models and policy. To answer this question, we show that, with the help of the CDC, the opponent models are more confident in predicting opponents’ actions, and the predictions are also more accurate. In turn, the CDC can assist the policy in identifying actions that yield more rewards, which results in better policies. Here, we also use the game PP–5v2 for demonstration. The results for the rest games are in the appendix (Figure A1). In the following, we provide evidence for each argument, respectively.

Opponent models are more accurate with CDC.

To prove that the opponent models are more accurate in predicting opponent actions with CDC, we adopt two metrics: 1). We compute the average entropy of the predicted probability distribution over opponent actions, which measures the confidence of the prediction. The less average entropy is, the more certain are the agents about the predicted opponent actions. 2). We compute the Kullback-Leibler (KL) divergence (Kullback and Leibler 1951) between the predicted and the true probability distribution over opponent actions. The KL divergence is the direct measure of the distance between the opponent models and the true opponent policies. The less the KL divergence is, the more similar are the opponent models to the true policies. Note that we only use the true opponent policies for evaluation. We do not use them to train DOMAC. From Figures 12(a) and 12(b), we conclude that the CDC can increase the training speed (faster descent) and improve the reliability and confidence (lower KL divergence and entropy) of the opponent models. Note that for the pommerman environment, we can not access the opponents’ policies but their actions instead due to the environment restrictions. Therefore, in Pomm–FFA and Pomm–Team games, we replace KL divergence with cross entropy loss (Zhang and Sabuncu 2018) which has a similar effect. The second argument, i.e., the CDC helps policy to identify actions with more rewards, is supported by the results in Figure 5 and 6, where the performance of DMAC is better than MAAC. Note that the expected returns of DMAC are still lower than DOMAC, which implies that the integration of OMA and CDC is essential for our method.

CDC helps policy to identify actions with more rewards.

This argument is supported by the results that DOMAC has the lowest entropy in Figure 12(c) and highest average episode rewards in Figure 5 and Figure 6. Furthermore, note that both OMAC and DMAC can also obtain a policy with a very low entropy after training. However, their expected returns are still lower than DOMAC, which means the actions they output with high confidence are not as good as those

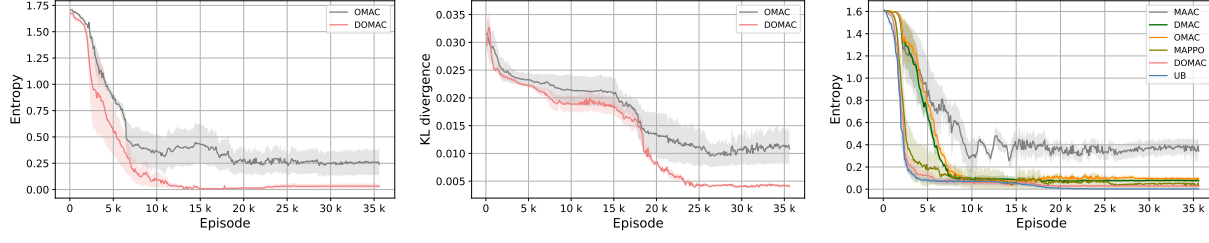
output by DOMAC. This implies that the integration of OMA and CDC is essential for our algorithm.

Conclusion and Future Work

This paper proposes a distributional opponent model aided actor-critic (DOMAC) algorithm by incorporating the distributional RL and speculative opponent models into the actor-critic framework. In DOMAC, the speculative opponent models take as input the controlled agents’ local observations, which realizes the opponent modelling when opponents’ information is unavailable. With the guide of the distributional critic, we manage to train the actor and opponent models effectively. Extensive experiments demonstrate that DOMAC not only obtains a higher average return but also achieves a faster convergence speed. The ablation studies and the baselines OMAC and DMAC prove that the OMA and CDC are both essential parts for our algorithm. That is, the CDC leads to a higher-quality OMA and in turn, the better OMA helps to improve the overall performance. Based on our above analysis, the proposed integration of OMA and CDC has the potential to improve the performance of various RL algorithms. For future work, we will study how to model opponents with dynamic strategies only using the local information. In addition, we plan to investigate extending DOMAC to value-based methods. By doing so, we will show that the integration of distributional reinforcement learning and opponent modelling can act as a general plugin that benefits a wide range of reinforcement learning algorithms.

References

- Albrecht, S. V.; and Stone, P. 2017. Reasoning about Hypothetical Agent Behaviours and their Parameters. In *Proceedings of the 16th Conference on Autonomous Agents and MultiAgent Systems*, 547–555.
- Albrecht, S. V.; and Stone, P. 2018. Autonomous agents modelling other agents: A comprehensive survey and open problems. *Artificial Intelligence*, 258: 66–95.
- Bai, W.; Zhang, C.; Fu, Y.; Peng, L.; Qian, H.; and Dai, B. 2023. PACER: A Fully Push-forward-based Distributional Reinforcement Learning Algorithm. *arXiv preprint arXiv:2306.06637*.
- Barth-Maron, G.; Hoffman, M. W.; Budden, D.; Dabney, W.; Horgan, D.; Dhruba, T.; Muldal, A.; Heess, N.; and Lillicrap, T. 2018. Distributed Distributional Deterministic Policy Gradients. In *International Conference on Learning Representations*.



(a) Average entropy of OM. (b) Average KLD of OM. (c) Average entropy of policies.

Figure 12: Impacts of the distributional critic on opponent models (OM) and policies for game PP-5v2.

- Bellemare, M. G.; Dabney, W.; and Munos, R. 2017. A distributional perspective on reinforcement learning. In *International Conference on Machine Learning*, 449–458. PMLR.
- Bellemare, M. G.; Dabney, W.; and Rowland, M. 2023. *Distributional reinforcement learning*. MIT Press.
- Brown, G. W. 1951. Iterative solution of games by fictitious play. *Activity analysis of production and allocation*, 13(1): 374–376.
- Claus, C.; and Boutilier, C. 1998. The dynamics of reinforcement learning in cooperative multiagent systems. *AAAI/IAAI*, 1998(746-752): 2.
- Dabney, W.; Kurth-Nelson, Z.; Uchida, N.; Starkweather, C. K.; Hassabis, D.; Munos, R.; and Botvinick, M. 2020. A distributional code for value in dopamine-based reinforcement learning. *Nature*, 577(7792): 671–675.
- Dabney, W.; Ostrovski, G.; Silver, D.; and Munos, R. 2018a. Implicit quantile networks for distributional reinforcement learning. In *International conference on machine learning*, 1096–1105. PMLR.
- Dabney, W.; Rowland, M.; Bellemare, M. G.; and Munos, R. 2018b. Distributional reinforcement learning with quantile regression. In *Thirty-Second AAAI Conference on Artificial Intelligence*.
- DiGiovanni, A.; and Tewari, A. 2021. Thompson sampling for Markov games with piecewise stationary opponent policies. In *Uncertainty in Artificial Intelligence*, 738–748. PMLR.
- Foerster, J.; Chen, R. Y.; Al-Shedivat, M.; Whiteson, S.; Abbeel, P.; and Mordatch, I. 2018a. Learning with Opponent-Learning Awareness. In *Proceedings of the 17th International Conference on Autonomous Agents and MultiAgent Systems*, 122–130.
- Foerster, J.; Farquhar, G.; Afouras, T.; Nardelli, N.; and Whiteson, S. 2018b. Counterfactual multi-agent policy gradients. In *Proceedings of the AAAI Conference on Artificial Intelligence*, volume 32.
- Foerster, J. N.; Chen, R. Y.; Al-Shedivat, M.; Whiteson, S.; Abbeel, P.; and Mordatch, I. 2017. Learning with opponent-learning awareness. *arXiv preprint arXiv:1709.04326*.
- Fu, H.; Tian, Y.; Yu, H.; Liu, W.; Wu, S.; Xiong, J.; Wen, Y.; Li, K.; Xing, J.; Fu, Q.; et al. 2022. Greedy when Sure and Conservative when Uncertain about the Opponents. In *International Conference on Machine Learning*, 6829–6848. PMLR.
- Gronauer, S.; and Diepold, K. 2022. Multi-agent deep reinforcement learning: a survey. *Artificial Intelligence Review*, 1–49.
- Grover, A.; Al-Shedivat, M.; Gupta, J.; Burda, Y.; and Edwards, H. 2018. Learning policy representations in multiagent systems. In *International conference on machine learning*, 1802–1811. PMLR.
- He, H.; Boyd-Graber, J.; Kwok, K.; and Daumé III, H. 2016. Opponent modeling in deep reinforcement learning. In *International conference on machine learning*, 1804–1813. PMLR.
- Hernandez-Leal, P.; Kartal, B.; and Taylor, M. E. 2019. A survey and critique of multiagent deep reinforcement learning. *Autonomous Agents and Multi-Agent Systems*, 33(6): 750–797.
- Hong, Z.-W.; Su, S.-Y.; Shann, T.-Y.; Chang, Y.-H.; and Lee, C.-Y. 2018. A Deep Policy Inference Q-Network for Multi-Agent Systems. In *Proceedings of the 17th International Conference on Autonomous Agents and MultiAgent Systems*, 1388–1396.
- Hu, J.; Harding, S. A.; Wu, H.; Hu, S.; and Liao, S.-w. 2020. Qr-mix: Distributional value function factorisation for cooperative multi-agent reinforcement learning. *arXiv preprint arXiv:2009.04197*.
- Huang, L.; Fu, M.; Rao, A.; Irissappane, A. A.; Zhang, J.; and Xu, C. 2022. A Distributional Perspective on Multiagent Cooperation With Deep Reinforcement Learning. *IEEE Transactions on Neural Networks and Learning Systems*.
- Iqbal, S.; and Sha, F. 2019. Actor-attention-critic for multiagent reinforcement learning. In *International Conference on Machine Learning*, 2961–2970. PMLR.
- Kim, D. K.; Liu, M.; Riemer, M. D.; Sun, C.; Abdulhai, M.; Habibi, G.; Lopez-Cot, S.; Tesauro, G.; and How, J. 2021. A policy gradient algorithm for learning to learn in multiagent reinforcement learning. In *International Conference on Machine Learning*, 5541–5550. PMLR.
- Kingma, D. P.; and Ba, J. 2015. Adam: A Method for Stochastic Optimization. In *ICLR (Poster)*.
- Koenker, R.; and Hallock, K. F. 2001. Quantile regression. *Journal of economic perspectives*, 15(4): 143–156.
- Konda, V. R.; and Tsitsiklis, J. N. 2000. Actor-critic algorithms. In *Advances in neural information processing systems*, 1008–1014.

- Kullback, S.; and Leibler, R. A. 1951. On information and sufficiency. *The annals of mathematical statistics*, 22(1): 79–86.
- Littman, M. L. 1994. Markov games as a framework for multi-agent reinforcement learning. In *Machine learning proceedings 1994*, 157–163. Elsevier.
- Liu, M.; Zhou, M.; Zhang, W.; Zhuang, Y.; Wang, J.; Liu, W.; and Yu, Y. 2019. Multi-Agent Interactions Modeling with Correlated Policies. In *International Conference on Learning Representations*.
- Lowe, R.; Wu, Y. I.; Tamar, A.; Harb, J.; Pieter Abbeel, O.; and Mordatch, I. 2017. Multi-agent actor-critic for mixed cooperative-competitive environments. *Advances in neural information processing systems*, 30.
- Lyu, X.; and Amato, C. 2020. Likelihood Quantile Networks for Coordinating Multi-Agent Reinforcement Learning. In *International Conference on Autonomous Agents and Multiagent Systems (AAMAS)*.
- Ma, X.; Xia, L.; Zhou, Z.; Yang, J.; and Zhao, Q. 2020. Dsac: Distributional soft actor critic for risk-sensitive reinforcement learning. *arXiv preprint arXiv:2004.14547*.
- Mnih, V.; Badia, A. P.; Mirza, M.; Graves, A.; Lillicrap, T.; Harley, T.; Silver, D.; and Kavukcuoglu, K. 2016. Asynchronous methods for deep reinforcement learning. In *International conference on machine learning*, 1928–1937. PMLR.
- Papoudakis, G.; Christianos, F.; and Albrecht, S. 2021. Agent Modelling under Partial Observability for Deep Reinforcement Learning. *Advances in Neural Information Processing Systems*, 34.
- Papoudakis, G.; Christianos, F.; and Albrecht, S. V. 2020. Local Information Opponent Modelling Using Variational Autoencoders. *arXiv preprint arXiv:2006.09447*.
- Papoudakis, G.; Christianos, F.; Schäfer, L.; and Albrecht, S. V. 2020. Benchmarking multi-agent deep reinforcement learning algorithms in cooperative tasks. *arXiv preprint arXiv:2006.07869*.
- Paszke, A.; Gross, S.; Chintala, S.; Chanan, G.; Yang, E.; DeVito, Z.; Lin, Z.; Desmaison, A.; Antiga, L.; and Lerer, A. 2017. Automatic differentiation in pytorch.
- Rabinowitz, N.; Perbet, F.; Song, F.; Zhang, C.; Eslami, S. A.; and Botvinick, M. 2018. Machine theory of mind. In *International conference on machine learning*, 4218–4227. PMLR.
- Raileanu, R.; Denton, E.; Szlam, A.; and Fergus, R. 2018. Modeling others using oneself in multi-agent reinforcement learning. In *International conference on machine learning*, 4257–4266. PMLR.
- Rashid, T.; Samvelyan, M.; Schroeder, C.; Farquhar, G.; Foerster, J.; and Whiteson, S. 2018. Qmix: Monotonic value function factorisation for deep multi-agent reinforcement learning. In *International Conference on Machine Learning*, 4295–4304. PMLR.
- Resnick, C.; Eldridge, W.; Ha, D.; Britz, D.; Foerster, J.; Togelius, J.; Cho, K.; and Bruna, J. 2018. Pommerman: A Multi-Agent Playground. *CoRR*, abs/1809.07124.
- Samvelyan, M.; Rashid, T.; De Witt, C. S.; Farquhar, G.; Nardelli, N.; Rudner, T. G.; Hung, C.-M.; Torr, P. H.; Foerster, J.; and Whiteson, S. 2019. The starcraft multi-agent challenge. *arXiv preprint arXiv:1902.04043*.
- Silver, D.; Lever, G.; Heess, N.; Degris, T.; Wierstra, D.; and Riedmiller, M. 2014. Deterministic policy gradient algorithms. In *International conference on machine learning*, 387–395. PMLR.
- Singh, R.; Lee, K.; and Chen, Y. 2020. Sample-based distributional policy gradient. *arXiv preprint arXiv:2001.02652*.
- Son, K.; Kim, D.; Kang, W. J.; Hostallero, D. E.; and Yi, Y. 2019. Qtran: Learning to factorize with transformation for cooperative multi-agent reinforcement learning. In *International conference on machine learning*, 5887–5896. PMLR.
- Sun, W.-F.; Lee, C.-K.; and Lee, C.-Y. 2021. DFAC framework: Factorizing the value function via quantile mixture for multi-agent distributional q-learning. In *International Conference on Machine Learning*, 9945–9954. PMLR.
- Sunehag, P.; Lever, G.; Gruslys, A.; Czarnecki, W. M.; Zambaldi, V.; Jaderberg, M.; Lanctot, M.; Sonnerat, N.; Leibo, J. Z.; Tuyls, K.; et al. 2017. Value-decomposition networks for cooperative multi-agent learning. *arXiv preprint arXiv:1706.05296*.
- Sutton, R. S.; and Barto, A. G. 2018. *Reinforcement learning: An introduction*. MIT press.
- Sutton, R. S.; McAllester, D. A.; Singh, S. P.; and Mansour, Y. 2000. Policy gradient methods for reinforcement learning with function approximation. In *Advances in neural information processing systems*, 1057–1063.
- Tessler, C.; Tennenholz, G.; and Mannor, S. 2019. Distributional policy optimization: An alternative approach for continuous control. *Advances in Neural Information Processing Systems*, 32: 1352–1362.
- Tian, Z.; Wen, Y.; Gong, Z.; Punakkath, F.; Zou, S.; and Wang, J. 2019. A regularized opponent model with maximum entropy objective. In *Proceedings of the 28th International Joint Conference on Artificial Intelligence*, 602–608.
- Wang, J.; Ren, Z.; Liu, T.; Yu, Y.; and Zhang, C. 2020. Qplex: Duplex dueling multi-agent q-learning. *arXiv preprint arXiv:2008.01062*.
- Wang, T.; Gupta, T.; Peng, B.; Mahajan, A.; Whiteson, S.; and Zhang, C. 2021. RODE: learning roles to decompose multi-agent tasks. In *Proceedings of the International Conference on Learning Representations*. OpenReview.
- Wen, Y.; Yang, Y.; Luo, R.; and Wang, J. 2019a. Modelling bounded rationality in multi-agent interactions by generalized recursive reasoning. *arXiv preprint arXiv:1901.09216*.
- Wen, Y.; Yang, Y.; Luo, R.; Wang, J.; and Pan, W. 2019b. Probabilistic recursive reasoning for multi-agent reinforcement learning. In *7th International Conference on Learning Representations, ICLR 2019*.
- Wiltzer, H. E.; Meger, D.; and Bellemare, M. G. 2022. Distributional Hamilton-Jacobi-Bellman equations for continuous-time reinforcement learning. In *International Conference on Machine Learning*, 23832–23856. PMLR.

Wu, Z.; Li, K.; Xu, H.; Zang, Y.; An, B.; and Xing, J. 2022. L2E: Learning to exploit your opponent. In *2022 International Joint Conference on Neural Networks (IJCNN)*, 1–8. IEEE.

Yang, T.; Hao, J.; Meng, Z.; Zhang, C.; Zheng, Y.; and Zheng, Z. 2019. Towards Efficient Detection and Optimal Response against Sophisticated Opponents. In *IJCAI*.

Yang, T.; Meng, Z.; Hao, J.; Zhang, C.; Zheng, Y.; and Zheng, Z. 2018. Towards efficient detection and optimal response against sophisticated opponents. *arXiv preprint arXiv:1809.04240*.

Yu, C.; Velu, A.; Vinitsky, E.; Gao, J.; Wang, Y.; Bayen, A.; and Wu, Y. 2022. The surprising effectiveness of ppo in cooperative multi-agent games. *Advances in Neural Information Processing Systems*, 35: 24611–24624.

Yu, L.; Qin, S.; Zhang, M.; Shen, C.; Jiang, T.; and Guan, X. 2021. A review of deep reinforcement learning for smart building energy management. *IEEE Internet of Things Journal*, 8(15): 12046–12063.

Yue, Y.; Wang, Z.; and Zhou, M. 2020. Implicit distributional reinforcement learning. *Advances in Neural Information Processing Systems*, 33: 7135–7147.

Zhang, D.; Pan, L.; Chen, R. T.; Courville, A.; and Bengio, Y. 2023. Distributional GFlowNets with Quantile Flows. *arXiv preprint arXiv:2302.05793*.

Zhang, K.; Yang, Z.; and Başar, T. 2021. Multi-agent reinforcement learning: A selective overview of theories and algorithms. *Handbook of Reinforcement Learning and Control*, 321–384.

Zhang, Z.; and Sabuncu, M. 2018. Generalized cross entropy loss for training deep neural networks with noisy labels. *Advances in neural information processing systems*, 31.

Zheng, Y.; Meng, Z.; Hao, J.; Zhang, Z.; Yang, T.; and Fan, C. 2018. A deep bayesian policy reuse approach against non-stationary agents. In *Proceedings of the 32nd International Conference on Neural Information Processing Systems*, 962–972.

Zintgraf, L.; Devlin, S.; Ciosek, K.; Whiteson, S.; and Hofmann, K. 2021. Deep Interactive Bayesian Reinforcement Learning via Meta-Learning. In *Proceedings of the 20th International Conference on Autonomous Agents and MultiAgent Systems*, 1712–1714.

Distributional opponent model aided policy gradient theorem

To clarify the idea of this work, we first compare the traditional MARL algorithms with the existing works on opponent modelling. Specifically, the traditional MARL algorithms use the information (observations and actions) of the controlled agents to train the team policy. These algorithms normally consider the opponents as a part of the environment. In comparison, the existing works on opponent modelling use opponent models to predict the goal/actions of the opponents so that the controlled team can make better decisions given those predictions. However, these opponent modelling works need to use the true information of the opponents to train the opponent models. In this work, we don't use the opponents' observations and actions to train the opponent model directly because we consider the setting where the opponent's information is inaccessible. That means our work tries to maintain the advantages brought by the opponent models while using the same information as the traditional MARL algorithms. However, this brings a challenge that we don't have the true opponent actions to act as the training signal of our opponent model. To find an alternative training signal, we propose to use the distributional critic. Because the distributional critic can provide the training signal for the controlled agent's actions while our controlled agent's actions are conditioned on the outputs of opponent models, the distributional critic enable the training of opponent models without true opponent actions.

In this work, we apply the distributional RL to the POMDP setting. Note that most of the existing works focus on the MDP setting, i.e., they use the global states as the input of the centralized critic while we use the joint observations instead. One may have the concern about whether it is feasible to learn with the joint observations. To address this concern, we would like to first clarify what a state s is. By definition, a state s is one configuration of all agents and the external environment. However, in practice, a state being used by the algorithms often cannot represent the configuration of external environment completely because there are many latent variables that can affect the state transition. For example, in Atari games, a state is an image that represents the current game status while the internal random seed of the simulator can affect the future states and it cannot be obtained by the learning algorithms. Therefore, when a learning algorithm takes a state as input, the state actually means the full information that is available to the algorithm. For the latent variables that the algorithm has no access to, we use the state transition function to depict the randomness brought by them.

In this sense, when learning the critic in POMDP setting, it is equivalent to MDP setting as long as the critic takes all available information (i.e., joint observation of all controlled agents) as input. Specifically, the return expectation of MDP setting is over the trajectories resulting from the state transition function $P(s'|s, a)$ and agent policies, i.e., $\mathbb{E}_{s \sim P(s'|s, a), a \sim \pi} [\mathbb{E}(Z(s, a))]$. Similarly, we can let the return expectation of POMDP setting to be over the trajectories resulting from the observation transition function $P(o'|o, a)$ and agent policies, i.e., $\mathbb{E}_{o \sim P(o'|o, a), a \sim \pi} [\mathbb{E}(Z(o, a))]$ (Equa-

tion (5) in our paper). Based on the state transition function $P(s'|s, a)$ and observation function $\mathcal{O}(o|s)$, we can define the observation transition function as

$$P(o'|o, a) = \sum_s P(s|o) \sum_{s'} P(s'|s, a) \mathcal{O}(o'|s'), \quad (20)$$

where $P(s|o) = \frac{P(s, o)}{P(o)} = \frac{P(s)\mathcal{O}(o|s)}{\sum_s \mathcal{O}(o|s)P(s)}$ according to the Bayesian theorem. Like in MDP, the observation transition function depicts the randomness brought by all unobservable information. Therefore, the return expectation of MDP and POMDP actually have the same mathematical form and they only use different transition functions to depict the randomness from unavailable information. In both settings, we can sample the trajectories for return estimation without explicitly learning the state transition function or observation transition function. Note that the return estimation in POMDP generally has more uncertainty than the return estimation has in MDP because POMDP has more unavailable information to introduce randomness in the observation transition function. This, however, necessitates the use of distributional critic to better cope with the return estimation uncertainty.

Environmental settings

Predator-prey: The states, observations, actions, and state transition function of each agent is formulated as below.

- **The observations.** Observations consist of high-level feature vectors containing relative distances to other agents and landmarks.
- **Actions space.** Any agent, either predators or preys, has five actions, i.e. [up, down, left, right, no-op] where the first four actions means the agent moves towards the corresponding direction by one step, and no-op indicates doing-nothing. All agents move within the map and can not exceed the boundary.
- **State transition \mathcal{T} .** The new state after the transition is the map with updated positions of all agents due to agents moving in the world. The termination condition for this task is when all preys are dead or for 500 steps.

Pommerman:

- **The states and observations.** At each time step, agents get local observations within their field of view 5×5 , which contains information (board, position, ammo) about the map. The agent obtain information of the Blast Strength, whether the agent can kick or not, the ID of their teammate and enemies, as well as the agent's current blast strength and bomb life.
- **Actions space.** Any agent chooses from one of six actions, i.e. [up, left, right, down, stop, bomb]. Each of the first four actions means moving towards the corresponding directions while stop means that this action is a pass, and bomb means laying a bomb.
- **Rewards \mathcal{R} .** In Pomm-Team, the game ends when both players on the same team have been destroyed. It ends when at most one agent remains alive in Pomm-FFA. The winning team is the one who has remaining members. Ties can happen when the game does not end before the

max steps or if the last agents are destroyed on the same turn. Agents in the same team share a reward of 1 if the team wins the game, they are given a reward of -1 if their team loses the game or the game is a tie (no teams win). They only get 0 reward when the game is not finished.

SMAC Setting:

- **The states and observations.** At each time step, agents receive local observations, which contain information (distance, relative x, relative y, health, shield, and unit type) about the map within a circular area for both allied and enemy units and makes the environment partially observable for each agent. The global state is composed of joint observations, which could be used during training. All features, both in the global state and in individual observations of agents, are normalized by their maximum values.
- **Action Space.** Any agent has the following actions, i.e., [up, left, right, down, attack, stop, no-op].
- **Rewards.** At each time step, the agents receive a joint reward equal to the total damage dealt to the enemy agents. In addition, agents receive a bonus of 10 after killing each opponent, and 200 after killing all opponents for winning the game. The rewards are normalized to ensure that the maximum cumulative reward achievable in each scenario is around 20.

Evaluation results

Analysis of the computation complexity

Intuitively speaking, training the speculative opponent model with local information seems more complicated and may need more data. To investigate whether the OMA and CDC can increase the computation complexity in our method, we provide the computational cost between different algorithms. We gather the number of floating-point operations (FLOPS) of a single inference and the number of parameters for each method. Table A1 shows the computation complexity of different algorithms. It shows that DOMAC has the comparable model volume and computational complexity as MAAC.

Table A1: Computational complexity in Pomm-Team

Algorithm	Params(M)	FLOPs(G)
MAAC	8.079	0.100
OMAC	8.085	0.101
DMAC	8.094	0.1005
DOMAC	8.100	0.1015

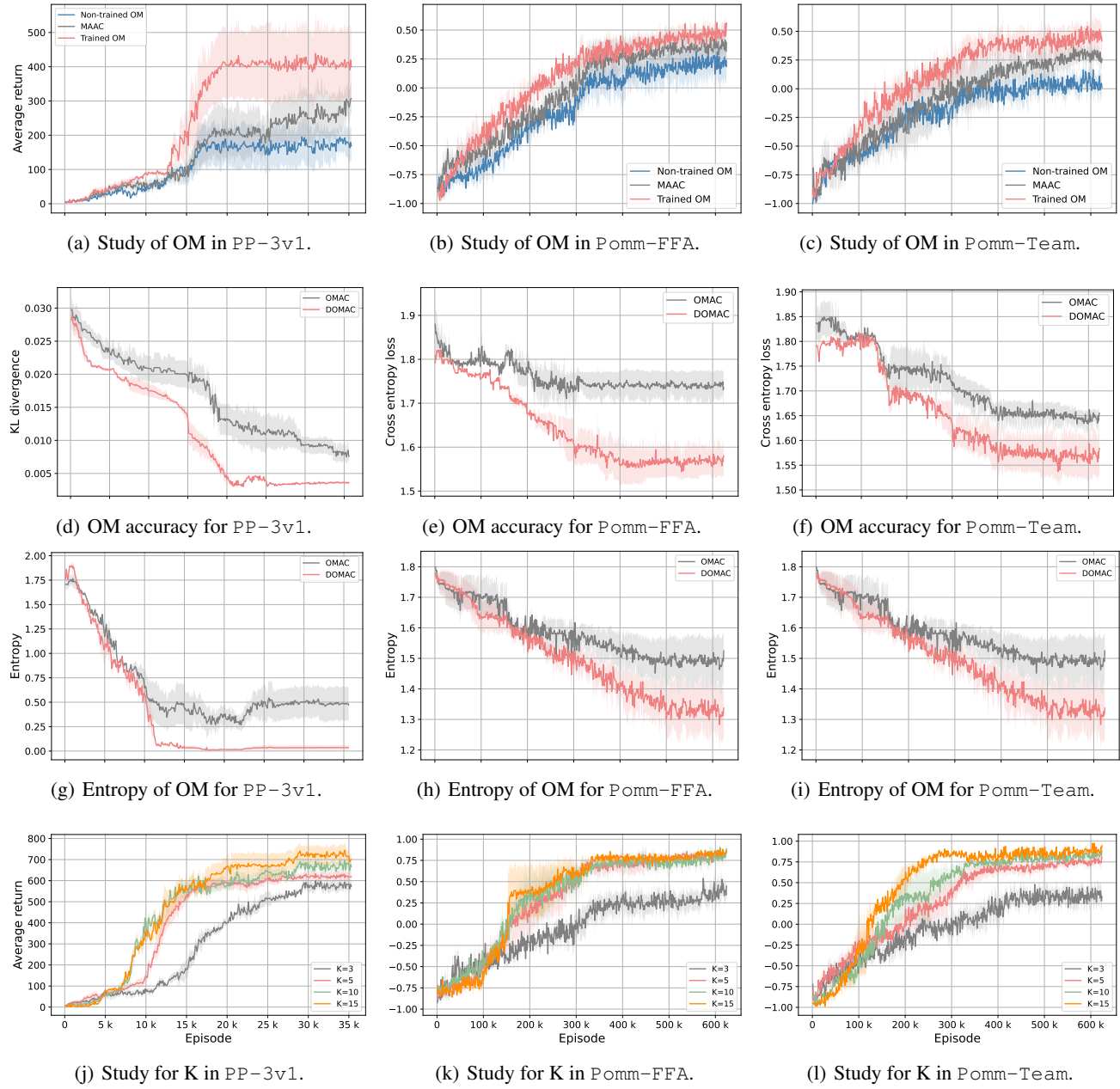


Figure A1: Ablation studies for opponent models (OM) and quantile number K in PP-3v1, Pomm-FFA, Pomm-Team.

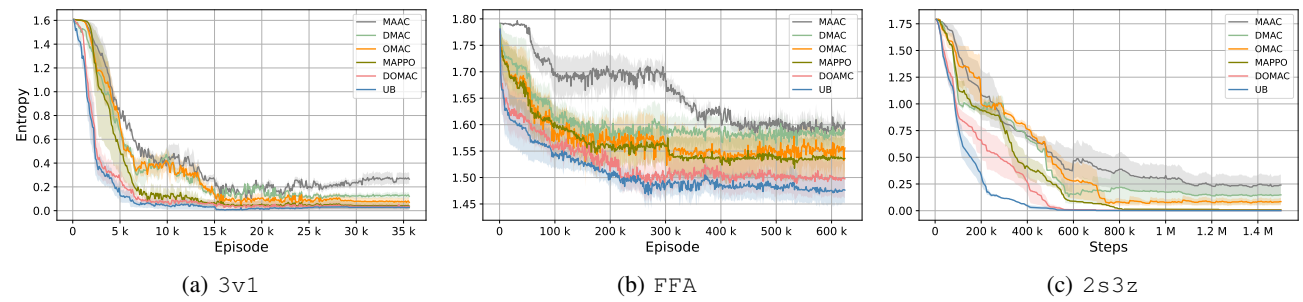


Figure A2: Average entropy of policies for game FFA and 2s3z.